EXPERIMENTAL RESIDUAL STRESS EVALUATION OF HYDRAULIC EXPANSION TRANSITIONS IN ALLOY 690 STEAM GENERATOR TUBING

Rod McGregor, Babcock & Wilcox International, Doug Hornbach, Lambda Research
Usama Abdelsalam, McMaster University, Paul Doherty, Babcock & Wilcox International

ABSTRACT

Nuclear Steam Generator (SG) service reliability and longevity have been seriously affected worldwide by corrosion at the tube-to-tubesheet joint expansion. Current SG designs for new facilities and replacement projects enhance corrosion resistance through the use of advanced tubing materials and improved joint design and fabrication techniques. Alloy 690TT tubing has demonstrated outstanding laboratory performance in accelerated primary water chemistries. Resistance to Secondary Water Stress Corrosion Cracking (SWSCC) has been shown to be generally superior to alternative materials. Full depth hydraulic expansion has largely replaced roller expansion in an effort to further reduce SWSCC susceptibility caused by secondary-side residual stress and cold work in the critical transition zone between the expanded and unexpanded tube. Study of the mechanics of the tubing under hydraulic expansion is of first order importance to understand and minimize residual stresses and cold work.

Transition zones of hydraulic expansions have undergone detailed experimental evaluation to define residual stress and cold work distribution on and below the secondary-side surface. Using x-ray diffraction techniques, with supporting finite element analysis, variations are compared in tubing metallurgical condition, tube/pitch geometry, expansion pressure, and tube-to-hole clearance. Initial measurements to characterize the unexpanded tube reveal compressive stresses associated with a thin work-hardened layer on the outer surface of the tube. The gradient of cold work was measured as 3% to 0% within .001" of the surface. The levels and character of residual stresses following hydraulic expansion are primarily dependent on this work-hardened surface layer and initial stress state that is unique to each tube fabrication process. Tensile stresses following expansion are less than 25% of the local yield stress and are found on the transition in a narrow circumferential band at the immediate tube surface (<.0002 inch/0.005 mm depth). The measurements otherwise indicate a predominance of compressive stresses on and below the secondary-side surface of the transition zone. Excellent resistance to SWSCC initiation is offered by the low levels of tensile stress and cold work. Propagation of any possible cracking would be deterred by the compressive stress field that surrounds this small volume of tensile material.

KEY WORDS

Hydraulic expansion, residual stress, stress corrosion cracking, Alloy 690.

INTRODUCTION

In a steam generator, the attachment of the tube to the tubesheet creates a barrier between the primary and secondary fluid circuits. In both a leakage sealing and structural capacity, the joint must sustain the forces of the applied differential pressures while not creating conditions that would cause the tube to degrade in-service through crevice corrosion or stress corrosion mechanisms. Joint designs have evolved based upon both analysis and experimentation and from study of in-service joint failures throughout the industry. Such observations have clearly identified susceptibility to Stress Corrosion Cracking (SCC) in susceptible tube materials at highly stressed locations on the tube, leading to leakage of primary coolant and requiring costly repairs or removal of the tube from service. The transition region between the expanded and unexpanded tube has been particularly problematic because of its higher tensile residual

stresses and its location at the tubesheet secondary-side where it is exposed to corrosive conditions that develop in the sludge pile (Figure 1).
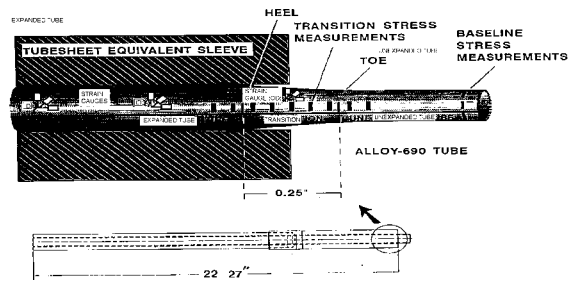

Fig. 1.

Based on the growing knowledge of tube degradation mechanisms, design and fabrication improvements to the joint have been incorporated into vessel designs for new and replacement projects. Full depth hydraulic expansion has largely replaced roller techniques in an effort to limit residual stresses. There have also been metallurgical advancements in both material composition and manufacturing which have resulted in superior grades of corrosion resistant tubing. Laboratory experiments that subject Alloy 690TT tubing to accelerated primary water chemistries have demonstrated outstanding performance and have provided a high level of confidence that the inside diameter (ID) residual stresses will not present a corrosion concern for this material.[1] However, at least one potential secondary-side environment (caustic plus lead) has been found to initiate cracking on the highly stressed Alloy 690 specimens in accelerated tests.[2] As a result, the outside diameter (OD) of the transition zone, where tensile stresses can exist, is not invulnerable to Secondary Water Stress Corrosion Cracking (SWSCC) throughout service life. Minimization of the OD surface residual stress is therefore of first order importance to both utilities and manufacturers in order to ensure reliability and longevity of new steam generator designs.

The hydraulic expansion process is amenable to analytical modeling as a 2D axisymmetric elastic-plastic problem. The behavior of the expansion, with particular attention to the character of the transition zone residual stress, has seen much attention analytically.[3,4] X-ray diffraction experimental techniques for study of hydraulically

expanded tubes have seen less attention in the literature. These can offer a more explicit understanding of the tubing metallurgical condition with its impact on the elastic-plastic mechanical behavior during the expansion process. In this study, a variety of expansion scenarios have been assessed using techniques for surface and subsurface residual stress and true plastic strain interpretation developed by Prevéy.[5] An evaluation is made of the initial stress state of the Alloy 690TT tubing for three distinct joint designs that use tubing fabricated by two unique processes. Surveys are conducted over the OD transition zone with variation in tube-to-hole clearance and expansion pressure. Supporting analysis using finite element (FE) modeling incorporates some of the unique features of the joint expansion process and qualities of the tubing revealed in the experimental program.

EXPERIMENTAL AND ANALYTICAL PROCEDURE

Tube-to-Tubesheet Joint Mockup Design

The residual stresses on the outside diameter of the hydraulic expansion transition are influenced by many variables in the material properties, geometries, and fabrication. The tube-to-tubesheet joint mockups have been designed to closely approximate three joint designs currently under fabrication for Advanced Series Replacement Steam Generators. The material properties and geometric parameters are described in Table I. Within the three joint designs (D1, D2, and D3), three tubesheet pitch sizes, two tube geometries and two methods of tubing fabrication (M1 and M2) are represented.

To simulate the tubesheet during the expansion process, the subject tubes are expanded into "equivalent sleeves[6]." The equivalent sleeve concept has been developed to simplify finite element modeling of hydraulically expanded joints. An accurate analytical representation of the joint depends on the accuracy of modeling the elastic response of the tubesheet during expansion pressure loading and unloading. Tubesheet elastic modulus and yield stress (Sy) are easily incorporated. Modeling of the perforated geometry, and the stiffening effect of

TUBE-TO-TUBESHEET JOINT GEOMETRIC, MATERIAL, AND FABRICATION PARAMETERS

Variable		Design #1 (D1)	Design #2 (D2)	Design #3 (D3)
TUBE	Outside Diameter	0.686 ± .001 inch (17.48 mm)	0.749 ± .001 inch (19.07 mm)	0.749 ± .001 inch (19.02 mm)
	Wall Thickness	0.039 inch (0.99 mm)	0.044 inch (1.12 mm)	0.044 inch (1.12mm)
	Material	Alloy 690	Alloy 690	Alloy 690
	Fabrication Process	(M1)	(M1)	(M2)
	S_y	43 ksi (296 MPa)	43 ksi (296 MPa)	43 ksi (296 MPa)
TUBESHEET	Equivalent Sleeve OD	1.294 inch (32.86 mm)	1.378 (35.00 mm)	1.422 (36.12 mm)
	Hole Diameter	.6955 + .005/-.004 inch (17.67 mm)	.758 + .005/-.004 inch (19.25 mm)	.758 + .005/-.004 inch (19.25 mm)
	Nominal Depth	27.13 inch (689 mm)	22.25 inch (565 mm)	25.5 inch (647 mm)
	S_y	67 ksi (461 MPa)	67 ksi (461 MPa)	67 ksi (461 MPa)
FABRICATION	Hydraulic Expansion Pressure	28.2, 33,2, 38.2 ksi (194, 229, 263 MPa)	27.8, 32.8, 37.8 ksi (191, 226, 260 MPa)	28.3, 33.3, 38.3 ksi (195, 229, 264 MPa)
	Crevice Depth	1/32 – 1/8 inch (0.8 – 3.2 mm)	1/32 – 1/8 inch (0.8 – 3.2 mm)	1/32 – 1/8 inch (0.8 – 3.2 mm)

Table I

expanded tubes that surround the expansion can be cumbersome. An empirical formula that provides an equivalent axisymmetric simulation is commonly applied.

In this study, the function and convenience of the equivalent sleeve is applied to the physical mockups as well as the analytical models. The sleeves, shown in Figure 1, were manufactured from SA-508 Class 3 material of yield strength equivalent to that of the subject tubesheets. The sleeve length is equivalent to the tubesheet depth to reproduce the foreshortening effect of the tube that occurs during the application of expansion pressure. Prototype hydraulic expansion mandrels were used and all steam generator production tooling and practices were reproduced during the expansion process.

The X-Ray Diffraction Technique

Strain in a crystalline material like Alloy 690TT will distort the interplanar lattice spacing. This change in spacing can be correlated to the change in diffraction angle of incident manganese Kα radiation from the (311) lattice planes of the face centered cubic (FCC) structure of this material. The diffracted radiation is received by a detector as a bell-curve distribution of intensity with respect to the diffraction Bragg angle. For two or more orientations of the sample, the angle of the peak of the intensity curve is measured using

Pearson VII fitting functions for the calculation of the stress value. The width of this diffraction peak is a sensitive function of the chemistry, hardness and the degree to which the material has been cold worked. A metal can be cold worked through bending, cutting, shot peening, grinding, or abrasion. Residual stresses remain on the plastically strained surface. In work-hardened materials, the diffraction peak width increases significantly as a result of an increase in the average microstrain and the reduced crystallite size produced by cold working. The (311) diffraction peak width can be indicative of how that material may have been processed, and through subsurface measurements, can reveal the depth to which it has been plastically deformed. The parameters and specifications of the techniques and equipment for the measurement of residual stresses and cold work distribution in nickel based alloys are discussed in detail in Reference 5.

Prior to x-ray diffraction residual stress measurements, removal of the mockup sleeve is necessary in order to provide access for the incident and diffracted x-ray beams. Electrical resistance strain gauge rosettes were applied at 0.25 inches (6.4 mm) and 0.5 inches (12.8 mm) from the secondary face of the inside diameter of the tube. The sleeve is carefully removed with two longitudinal saw cuts. The measured strains in the tube from the release of the sleeve are used in combination with a linear finite

element model to determine the stress relaxation which occurred on the outside diameter of the tube. The calculated relaxation from sectioning was used to correct the x-ray data measured in the hoop and axial direction over the transition between the expanded and unexpanded tube. The final residual stress value has an error of ±4 ksi (±28 MPa).

As an initial exploratory, X-ray diffraction measurements were made on the as-received surface and subsurface of the tubing samples from each of the two fabrication methods. These results would serve to confirm the validity of the technique by comparison with residual stress data supplied by the manufacturer. Measurements were also made at the apex of C-rings manufactured from Alloy 690TT and Alloy 600TT tubing and loaded to produce a 20 ksi (138 MPa) peak stress in accordance with ASTM G38. Comparison of the X-ray diffraction measured stresses with the objective C-ring apex stress values will provide further support to the accuracy of the technique on 600 series alloys.

Finite Element Analysis

To assist in the interpretation of the experimental residual stress data, a program of finite element modeling was undertaken. As an analytical problem, the hydraulic expansion of the tube-to-tubesheet joint is complex and highly non-linear. This non-linearity arises from three distinct sources: material non-linearity because of the elastoplastic behavior, geometric non-linearity due to the large strains and displacements, and finally the boundary condition non-linearity as a result of the contact interaction between the tube outer surface and the sleeve bore. Each of these non-linearities has to be dealt with carefully in order to obtain useable and reliable results systematically. An incremental technique is adopted in the INDAP finite element code developed by Dokainish.[7] The problem is approximated as a collection of piece-wise linear load steps where the solution is obtained iteratively at the boundaries of these load steps.

The tube expansion models developed are 2D axisymmetric geometries corresponding to the subject tubes within their equivalent sleeves. The INDAP code applies an elastic-plastic material model and kinematic work hardening coefficient to models incorporating unique features of the design and expansion process of the physical mockups. The models contain 380 isoparametric quadrilateral 9-node elements and 1700 nodes. To account for

expected stress gradients, the mesh is refined at the OD surface and around the transition region.

RESULTS AND DISCUSSION

Test Series 1 - Surface and Subsurface Stress Measurements on As-Received Tubing and C-Rings
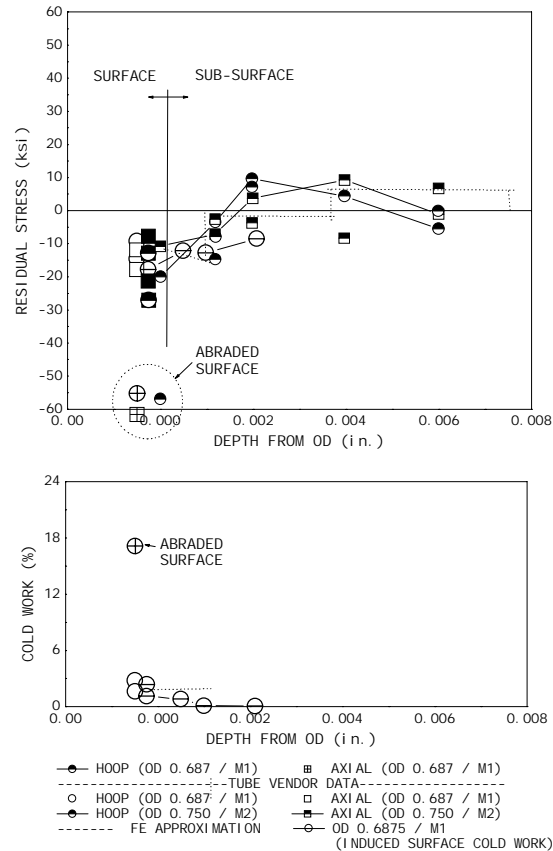

Fig. 2(a) – Alloy 690TT tubing: surface and through-wall residual stress and % cold work.

Figure 2(a) shows the residual stress variation on the surface and through the wall thickness of the tubing material from both methods of manufacture. X-ray diffraction data from this study and from the tubing vendor are presented together showing close correlation. The M1 tubing in the fire shows a compressive surface stress from -8 to -16 ksi (-55 to -110 MPa) with somewhat higher magnitudes in the axial stress direction. The M2 tubing shows more scattered compressive stress values on the surface from -7 to -26 ksi (-48 to -179 MPa) with no consistent dominance in the hoop or axial direction.

Experimental Residual Stress Evaluation of Hydraulic Expansion Transitions in
Alloy 690 Steam Generator Tubing

In all cases shown in Figure 2(a), a gradient of residual stress is apparent. Surface compressive stresses reduce within 0.002 inch (0.050 mm) of the OD and are balanced by mild tensile stresses (~10 ksi) that relax to a relatively stress-free state around 0.006 inch (0.150 mm) of depth. The experimental interpretation of the cold work profile within the tube wall indicates the existence of a work-hardened surface layer that is causing this residual stress profile. A typical M2 tube displays a plastic strain gradient from 2% to 0% within 0.001 inch (0.025 mm) of the surface. The M1 tubing indicates comparable surface cold work with a level that is closer to 3%. The tubing thermal treatment is the final stage to the fabrication and is controlled for the function of grain boundary carbide precipitation. As such, it does not fully relieve the stresses from the surface grinding and other cold reduction operations. The M1 and M2 tubing are the products of different cold reduction processes that could account for the distinct character and magnitudes of the surface stresses and work-hardened state.

Figure 2(a) also illustrates the development of compressive surface stress through the induced cold work of abrasive paper surface conditioning (to 17% from the initial state of 3%). Similar to the beneficial effect of shot peening, the indicated compressive stress increase from around 12 to 60 ksi (83 to 413 MPa) should be protective against stress corrosion effects in the tube freespan. However, any such strain hardening of the surface layer, including that shown to be induced by the manufacturing processes, changes the S_y locally and will influence the surface stresses following hydraulic expansion.

The results of the C-ring apex X-ray diffraction measurements are included in Figure 2(b). Measured stresses are only about 5 ksi (34 MPa) where 20 ksi (138 MPa) was predicted based on the assumption of a homogeneous metal with a 0 ksi stress at the surface. Because the C-ring flexure is a linear-elastic strain, the effect is shown of adjusting the measured stresses with respect to the initial surface stress data of 15 ksi (107 MPa) for the Alloy 690 TT tubing. In fact, a stress differential of 20 ksi (138 MPa) was induced; thus providing additional confirmatory evidence for the validity of the X-ray diffraction technique for this application. The surface stress which is effecting the measured magnitude on the elastically deformed C-rings will also influence results following the elastic and plastic deformations that are induced on the surface of the transition zone by hydraulic expansion.
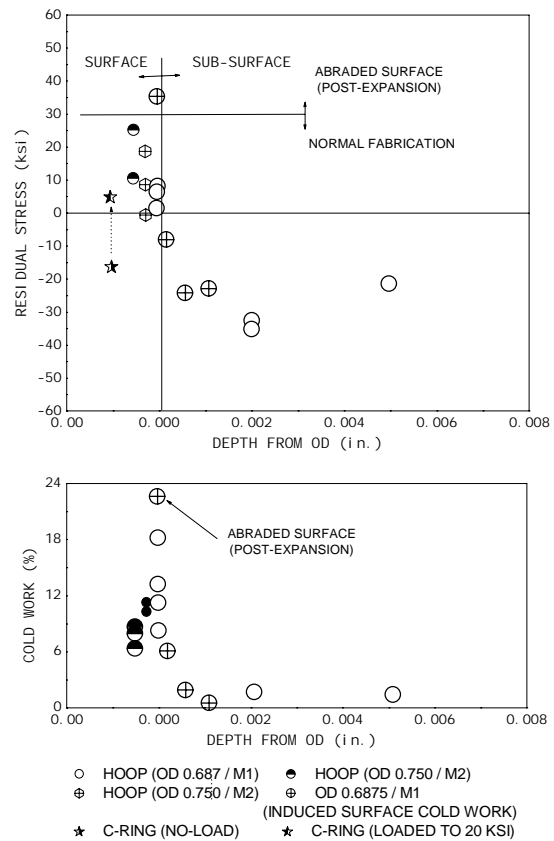

Fig. 2(b) – Hydraulically expanded alloy 690TT tubing: surface and through-wall residual stress/cold work variation measured from the OD transition zone tensile peak location.

Test Series 2 - Hydraulic Expansion Transition Residual Stresses on Nominal Fabrications and Geometric Tolerance Extremes

Typical transition zone residual stress surveys are shown in Figures 3 and 4 for two of the three expansion scenarios (D1 and D3) representing the M1 and M2 tubing, along with the finite element prediction. For both hoop and axial directions the pattern of stress distribution was shown to be similar for each tubing type and closely predicted by the analysis, particularly for M2 expansion shown in Figure 4. The location of the hoop stress peak is the end result of a complex interaction and equilibration of elastic and plastic deformations within a small axial length of the thin walled tube. The hoop stress peak tends to be limited to a narrow circumferential band (< 0.1", 2.5 mm) at the middle of the slope between the so called "heel" and "toe" of the transition zone. The location of the axial stress peak (which remains compressive for M1 tubing) is

---

Experimental Residual Stress Evaluation of Hydraulic Expansion Transitions in
Alloy 690 Steam Generator Tubing

somewhat more intuitive; it is found closer to the heel location where bending stresses would be expected.

FIGURE 3(a)
RESIDUAL STRESS/PROFILE (EXPMT.)

FIGURE 3(b)
RESIDUAL STRESS/PROFILE (FE ANALYSIS)

% STRAIN = 2.0

% STRAIN = 0.0

FIGURE 3(c)
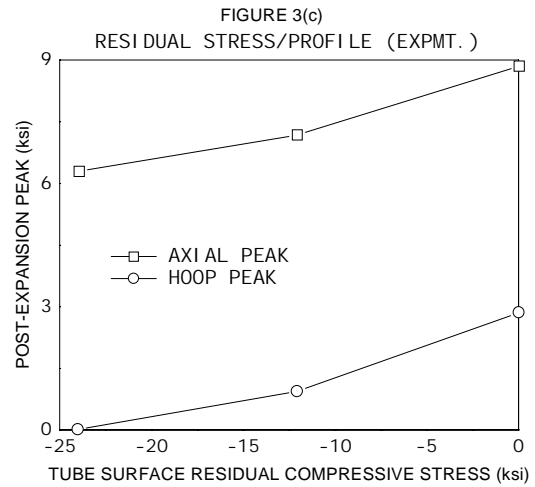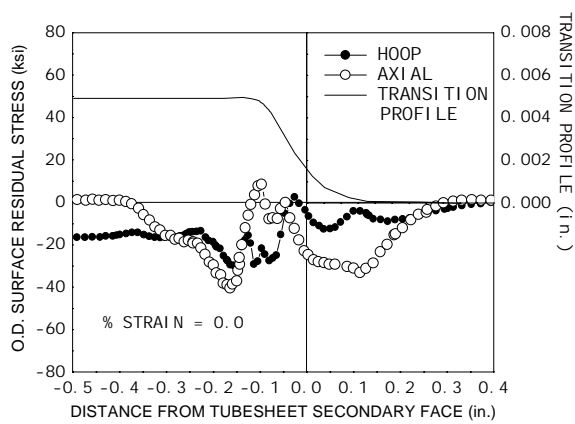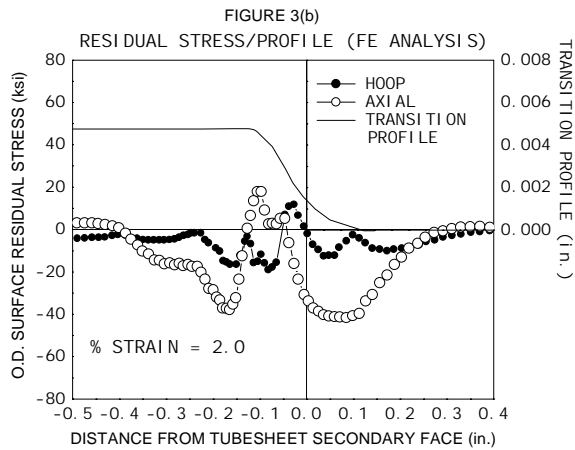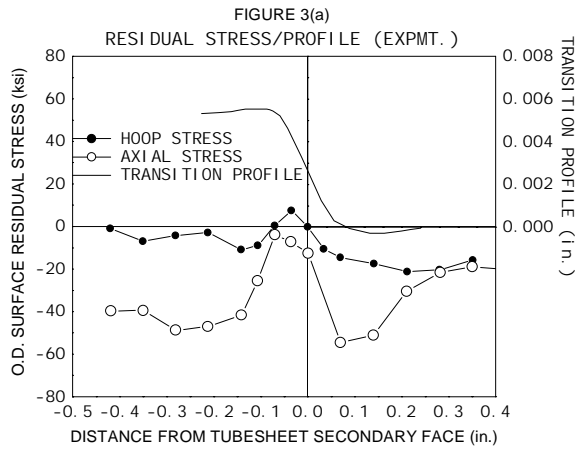RESIDUAL STRESS/PROFILE (EXPMT.)

Fig. 3(a), (b), (c) – M1 / D1 hydraulic expansion: x-ray diffraction and finite element residual stress/cold work and physical profiles over transition OD. Tube geometry – OD = 0.6875 in., wall = 0.039 in. Tube to hole clearance - .0045 (± .0005) in. radial. Hydraulic expansion pressure – 33,200 psi.

The direction of the tensile stress-peak is significant because of its relation to the direction of potential cracks. The D1 and D2 joint designs both use tubing of the same fabrication process (M1) of different geometric specifications (OD and wall thickness). Both D1 and D2 expansions display experimental stress distributions as shown in Figure 3(a) where there is a consistent dominance of hoop stress over the transition with no tensile levels at all in the axial stress direction. The D3 design used M2 fabricated tubing which is geometrically identical to the M1 tubing used in D2. The character of the experimental hoop and axial stress distribution is distinctly different for the expanded M2 tubes which show tensile axial stresses with peak levels that are similar to the hoop stress peaks as shown in Figure 4. This remains true when the M2 tubing is expanded into the D2 sleeve. This exercise eliminated pitch or hydraulic expansion variables, leaving differences between the M1 and M2 tubing as the likely source of this observed difference in stress character.

Since the elastic modulus and Sy of the M1 and M2 materials are essentially the same, FE modeling has been used to explore the influence of the work-hardened surface layer and skin stresses that were shown to be unique to the M1 and M2 tubes. A

Experimental Residual Stress Evaluation of Hydraulic Expansion Transitions in
Alloy 690 Steam Generator Tubing

work-hardened surface layer was imposed on the analytical tube model by increasing the Sy in the surface elements in accordance with an Alloy 690 true stress/strain curve and using the experimentally measured cold work value of 2% from Figure 2(a). Figure 3(b) shows the tendency towards higher post-expansion tensile stresses as a function of the increase in the level of strain hardening on the initial tube surface. The FE model was then used to study the influence of the residual stresses associated with the work-hardened surface layer. In Figure 2(a) these were shown to be scattered but unique in character to each tube fabrication. As was observed following the elastic deformation of the C-rings in Test Series 1, the surface stresses were also found to influence the stress profiles following the plastic deformation of hydraulic expansion. Compressive stress added to the surface elements of the tube in each of the hoop and axial directions tended to decrease their corresponding stress peaks following hydraulic expansion as shown in Figure 3(c). The unique stress characters on the transition of the M1 and M2 tubing appear to be caused by both the work-hardening and the residual stresses on the tube surface as they influence the elastic-plastic deformation and equilibration during the expansion process. This phenomenon has been previously reported by Scott et al.[8]

Figure 2(b) shows additional evidence of the effect of initial surface skin stress on the post-expansion surface stress. The two subsurface profiles were measured at the tensile stress peak location on an expansion of a typical tube (with 3% cold work) and a tube subjected to severe conditioning of the surface using abrasive paper (to 17% cold work). The latter is an extreme cold worked condition, created as an exercise to emphasize the effect on the stresses before and after expansion. The magnitudes of the induced cold work and surface stresses in the unexpanded tube are shown in Figure 2(a). The compressive stress on the surface of a typical tube creates a tensile stress peak (< 20 ksi/138 MPa) following expansion. The heavily cold worked surface layer produces a much higher (36 ksi/248 MPa) level of tensile stress following hydraulic expansion. From the normal and abraded condition data presented in Figure 2(b), it appears that the surface tensile stress that is induced by the expansion is very thin (less than 0.0002"). Stresses reduce rapidly to high compressive levels that approach -30 ksi (-207 MPa). Crack propagation is arrested by material under compressive stress.
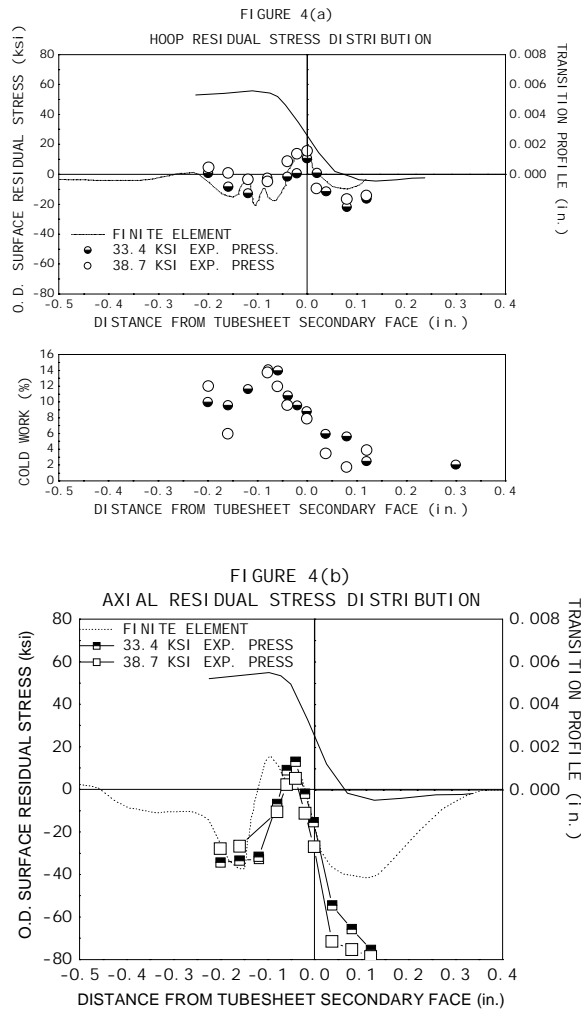

FIGURE 4(a)
HOOP RESIDUAL STRESS DISTRIBUTION

FIGURE 4(b)
AXIAL RESIDUAL STRESS DISTRIBUTION

Fig. 4 (a), (b) – M2 / D3 hydraulic expansion: x-ray diffraction and finite element residual stress/cold work and physical profiles over transition OD. Tube geometry – O.D. = 0.750 in., wall – 0.043 in., tube to hole clearance - 0.0045 (± .0005) in. radial, hydraulic expansion pressure – 33,400 and 38,700 psi.

A work-hardened surface will have a higher Sy than the base material. While the tube is expanding, the hardened surface remains elastic longer than the underlying metal and then proceeds to strain harden to a different extent. When the hydraulic expansion pressure is relieved, the tubesheet sleeve retracts and clamps the tube by forcing it beyond its relaxed equilibrium state. This elastically compresses the tube material and its surface layer in accordance with different stress strain relationships to a new equilibrium with the contracting tubesheet. In addition to the elevated residual stress that has been observed on the surface layer, the associated true plastic strain has been measured at around 12% (Figure 2(a)). At 0.002 inch (0.050 mm) beneath the surface, 0.8% to 2.8% cold work are indicated for

production typical expansions. This corresponds to the calculated strain of 2.2 ± 0.2% based on the known circumferential dimension increase in the expanding tube at this depth. Plastic strain from the expansion process alone is therefore more closely reflected in the levels measured immediately below the work-hardened surface.

The magnitudes of residual tensile stresses within this thin surface layer are low for all fabrications - generally less than 15 ksi (103 MPa). Repeated tests, however, show that the data can be widely scattered as a direct result of the cold work and surface stress variation in the as received tube. Scatter will be influenced to a lesser extent by variability in the expansion mandrel hydraulic seal compression characteristics, hydraulic expansion pressure variation, and small geometric/metallurgical variations in the tube and tubesheet sleeve. Repeated tests on production typical mockups have predicted stresses as high as 19 ksi (131 MPa) for an M1 tube. From an Alloy 690TT true stress strain curve, an Sy gradient from the surface can be approximated from the measurement of plastic strain. This maximum residual stress magnitude is 25% of the local (surface) Sy and less than 45% of the initial tube Sy. For Alloy 690 TT material, such levels are considered to be low relative to evidence of SCC threshold stress for this material. These suggest that magnitudes near 100% Sy are required to initiate cracking in high caustic concentrations.[1,2,9]

Test Series 3 - Out-of-Tolerance Hole Size and Expansion Pressure

In Figures 5 and 6, variation in the peak stresses are compared with respect to changes in tube-to-hole clearance and expansion pressure - both within and beyond fabrication tolerance. The data are widely scattered as a result of variation in the surface stress state on the as-received tube. In both cases, the hoop stress does not seem to show a significant increase. The axial stress tends to increase only as a function of tube-to-hole clearance. Cold work trends are demonstrated by levels measured at the stress peak locations. As discussed, cold work magnitudes below the work-hardened surface layer are substantially lower than the surface values shown in these figures. Increasing the tube-to-hole clearance, results in a general increase to the cold work in the metal from 12% to 26% as illustrated in the figure at the stress peak location. The dilation of the tube that is induced by a clearance increase of 0.002 inch (0.050 mm), is an order of magnitude greater than the dilation caused by expansion pressure increase. Expansion pressure

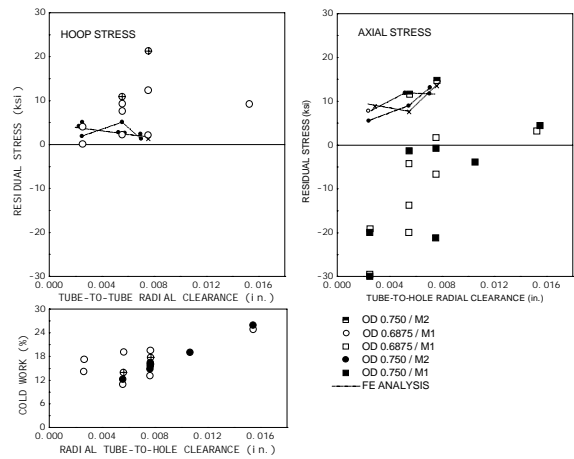increase, therefore, shows minimal effect on the cold work and residual stress in the transition.

Fig. 5 – Hydraulic expansion transition peak tensile residual stress variation vs. tube-to-hole radial clearance.
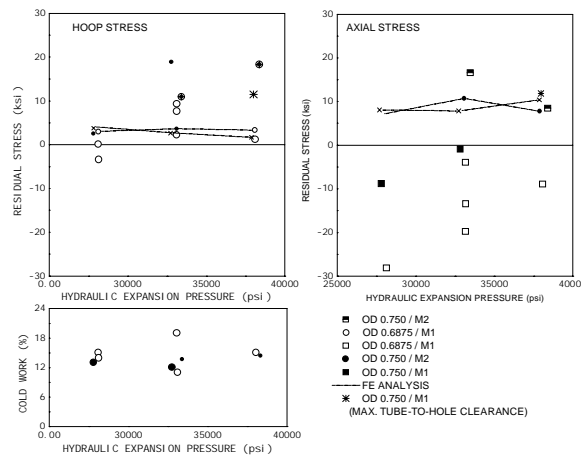

Fig. 6 – Hydraulic expansion transition peak tensile residual stress variation vs. hydraulic expansion pressure.

CONCLUSIONS

X-ray diffraction has been used to measure surface and subsurface residual stresses and cold work on steam generator tubes. Measurements were made on the material in the as-received state, ASTM G38 C-rings, and on the outer surface and subsurface of hydraulic expansion transitions of tube-to-tubesheet joint mockups. Several fabrication variables were examined with the support of finite element modeling. The significant findings are as follows:

1. The levels of surface residual stress measured on the expansion transition surface are closely dependent on variations in the work-hardened surface and residual stresses on the unexpanded tube. Typical surface ground tubes have surface compressive stresses from -4 to -26 ksi (-28 to -179 MPa) corresponding to around 3% cold work that relaxes to 0% cold work within .001" of the surface. The character of work-hardened surfaces is dependent on processing and cold reduction steps that are unique to the tube fabrication process.

2. The tensile stress field on the expansion transition surface extends for less than 0.1" (2.5 mm) of axial tube length and has a peak level that varies from 0 to 19 ksi (0 to 131 MPa) which is less than 25% of the local S_y. Subsurface measurements reveal a rapid decline from any magnitude of surface tensile stress resulting in fully compressive stresses within .0002 inch (0.0050 mm) of the surface extending to at least 0.005 inch (0.125 mm) below the surface. Considering the low magnitude of tensile skin stress within this narrow band combined with the crack arresting effect of the compressive stress that exists immediately below the surface, excellent resistance to SWSCC initiation and propagation is indicated for these expansions.

3. Beyond typical data scatter, there is no apparent difference in the levels of OD surface residual stress as a function of the three typical PWR tube/pitch geometries, or the range of tube-to-hole clearances or expansion pressures evaluated. SWSCC susceptibility is therefore not significantly influenced by these design variables.

REFERENCES

1. Norring, K., Engström, J and Törnblom, H., "Intergranular Stress Corrosion Cracking in Steam Generator Tubing. 25000 Hours Testing of Alloy 600 and Alloy 690," Fourth International Symposium on the Degradation of Materials in Nuclear Power Systems - Water Reactors, (Jekyll Island, Georgia, August 6-10, 1982, pg. 12-1).

2. Briceno, D. Castano, M. and Bollini, G., "Inconel 690 TT and Incoloy 800 in S, Cu and Pb Environments," EPRI Workshop Steam Generator Secondary IGA/SCC. (Reston, Va: 1991).

3. Hwang, J., Harrod, D., and Middlebrooks, W., "Analytical Evaluation of the Hydraulic Expansion of Steam Generator Tubing into Tubesheets," International Conference of Expanded and Rolled Joint Technology, Paper C.10 (Toronto, Ontario: Canadian Nuclear Society, 1993).

4. Updike, D., Kalnins, A., and Caldwell, S., "Residual Stresses in Transition Zones of Heat Exchanger Tubes," PVP - 175, 1989.

5. Prevéy, P., "The Measurement of Subsurface Residual Stress and Cold Work Distributions in Nickel Base Alloys," Residual Stress in Design, Process and Materials Selection, (pp. 11-19, ASM International Conference Proceedings, 1987).

6. Chaaban, A., Ma, H., and Bazerqui, A., "Tube-to-Tubesheet Joint: A Proposed Equation for the Equivalent Sleeve Diameter Used in the Single Tube Model," PVP Conference, (San Diego, Ca: ASME, 1991).

7. Dokainish, M., INDAP Theoretical Manual, Mechanical Engineering Department, McMaster University, 1988.

8. Scott, D., Wolgemuth, G., and Aiken, J., "Journal of Pressure Vessel Technology," Vol. 106 (1984).

9. Dominion Engineering, Inc., Guidelines for PWR Steam Generator Tubing Specifications and Repair, EPRI NP-6743-L, Volume 2, Project S408-1, February 1991.